Chemisorption of group-III metals on the (111) surface of group-IV semiconductors: In/Ge(111)

Zheng Gai, R. G. Zhao, Yi He, Hang Ji, Chuan Hu, and W.S. Yang*
Department of Physics and Mesoscopic Physics Laboratory, Peking University, Beijing 100871, China
(Received 16 June 1995)

We have studied the surface reconstructions of the In/Ge(111) system by means of scanning tunneling microscopy, low-energy electron diffraction, and Auger electron spectroscopy. In atoms at the interface substitute the top-layer Ge atoms at all coverages and tend to relax downward, thus causing a compressive surface stress. To release the stress, some of the top-layer Ge atoms may be missing and some new lateral bonds may form between the second-layer Ge atoms. Depending on the concrete way of stress relief, which may vary with the In coverage, different surface reconstructions may form. Detailed atomic structural models for the striped and hexagonal structures of the system have been proposed for further studies. Comparing the information gathered from previous papers concerning the systems of group-III metals adsorbed on (111) surfaces of group-IV semiconductors, we suggest that the above mechanism might also be responsible for formation of the reconstructions of the III/IV(111) systems in general, at least when the coverage is around 0.5 ML.

I. INTRODUCTION

It is well known that metal adsorbates may induce reconstructions of semiconductor surfaces.[1] Among all metal/semiconductor interface systems the group-III–metal/Si(111) systems might be of most studied, so far.[2–31] Besides, the group-III–metal/Ge(111) systems have been receiving more and more attention.[32–39] As a result of the great many experimental and theoretical efforts,[2–16] the simplest reconstruction of the systems, i.e., the $(\sqrt{3}\times\sqrt{3})$ $R30°$ structure with $\frac{1}{3}$ monolayers (ML) of metal has been known quite well. In contrast, much less has been understood and there seems to be no general consensus on the characterization of the reconstructions with higher coverages, which, however, seems to be more closely related to formation of the interfaces between group-III metals and group-IV semiconductors.[17] Motivated by this status, the present work has studied the surface reconstructions induced by indium adsorbed on the Ge(111) surface by means of the STM (scanning tunneling microscopy), LEED (low-energy electron diffraction), and AES (Auger electron spectroscopy). In an earlier RHEED (reflection high-energy electron diffraction) investigation of the In/Ge(111) system[36] the phase diagram of the surface reconstructions has been carefully determined and models of the effective scattering factors of "abnormal atoms," which should be very useful for further determination of the atomic structures of the reconstructions, have been proposed. Very recently, the system was studied with STM, LEED, and AES,[37] and many structural details of its reconstructions have been disclosed. In the present paper, on the basis of the dual-bias high-resolution STM images we obtained, concrete structural models of the surface reconstructions of the system is proposed and discussed. Combining the information obtained from the present STM investigation of the In/Ge(111) system with those gathered from the published papers concerning the Al/Si(111),[17–21] Ga/Si(111),[22–25] In/Si(111),[26–31] Al/Ge(111),[32] Ga/Ge(111),[33–35] and In/Ge(111) (Refs. 36–39) systems, a unified understanding of the medium-metal-coverage (around 0.5 ML) phases of group-III metals on the (111) surface of group-IV semiconductors emerges and will be discussed also.

II. EXPERIMENT

The experiment was carried out in two UHV systems. The first one was reported earlier[40] and consisted of a sample preparation chamber and a main chamber equipped with LEED, AES, and electron-energy-loss spectroscopy. The second system was reported and used earlier[41] and consists of a sample preparation chamber and a main chamber equipped with STM, LEED, and AES. The home-made STM, which is the same as that used in previous studies,[42] is suspended by four 50-cm-long springs in the vacuum system that is set on a vibration isolation box filled with layers of sand and sawdust. The sample with a size of $7\times7\times0.5$ mm^3 was cut from an Sb-doped Ge(111) wafer (18–20 Ωcm). After Ar^+ bombardment (5×10^{-5} Torr, 600 V, 1.5 h) and annealing (800 °C, 15 min) a clean and well-ordered Ge(111)-$c(2\times8)$ surface was always obtained, as verified by the sharp LEED pattern and the very small AES signals of O and N, i.e., the O(503 eV)/Ge(47 eV) and N(379 eV)/Ge(47 eV) ratios being below 3×10^{-4}. The In source was calibrated and used in a previous work,[41] which consisted of a piece of In (99.999%) wrapped with a Ta ribbon that was heated by an ac current passing through it. In was deposited with a rate of 0.12 ML/min onto the clean Ge(111)-$c(2\times8)$ surface at room temperature. 1 ML (7.22×10^{14} atoms/cm^2) was calibrated to correspond to an In(404 eV)/Ge(1147 eV) AES ratio of 4.8. The constant-current mode was used throughout the STM work. The bias was applied to the sample and

the tip was grounded. The tip was made out of tungsten wire with electrochemical etching.

III. EXPERIMENTAL RESULTS

We have studied the reconstructions in the entire range of the In coverage and annealing temperature that Ref. 36 studied, namely, the coverage up to 2 ML and the temperature up to 800 °C. Our results confirmed the phase diagram, except the $(\sqrt{61} \times \sqrt{61})R(30 \pm 4°)$ structure.[36] With STM we were never able to find any place where only one reconstruction exists, although usually one was dominant.

Below 0.4 ML of In, the α structures[36] or the striped phase[37] were observed with the STM. Several typical STM images are shown in Fig. 1, which are actually very similar to those published previously.[37] In the empty-state images long and thin domains consisting of two or more $2\sqrt{3}$ rows of bright round features are separated by darker domain boundaries with a width of 12.0 Å (three times the substrate unit length). In the boundaries a zigzag structure with a period of $2\sqrt{3}$ can be vaguely seen. In the filled-state images the domains look like $2\sqrt{3}$ rows of twins (not always resolvable) of bright round features, while the boundaries now look like $2\sqrt{3}$ rows of bright round features with similar brightness as that of the features in the domains. It is interesting that the widths of the domains fluctuate and the averaged widths increase with decreasing In coverage, while the width of the boundaries, in contrast, remains three times that of the substrate unit length.

Shown in Figs. 2(a) and 2(b) are two typical STM images collected from the surface with an In coverage of 0.4 to 0.7 ML, which gave sharp $(4\sqrt{3} \times 4\sqrt{3})R30°$ LEED patterns with a low background [Fig. 2(c)]. Surprisingly, the surface looked to be not very well ordered, at least not as good as what one would expect from its LEED patterns. However, a comparison of the FFT [two-dimensional fast Fourier transform, Fig. 2(d)] of the STM image [Fig. 2(a)] with the LEED pattern indicates that both techniques indeed studied the same structure. In the empty-state images each $(4\sqrt{3} \times 4\sqrt{3})$ unit cell contains three similar groups of bright spots, which approximately form a (1.15×1.15) local order, separated by darker group boundaries. The shape of the groups and the number of the bright spots contained in each group varies more or less, similar to the published images of the hexagonal phase.[37] In the filled-state images, the contrast compared to that of the empty-state images is completely reversed, i.e., the dark spots approximately form a (1.15×1.15) local order within the groups that are separated by brighter boundaries. From Figs. 2(c) and 2(d) we see that the bright fractional-order beams form patches near the integral-order beams rather than spread everywhere. From the distribution of the fractional order beams it is estimated that the $(4\sqrt{3} \times 4\sqrt{3})$ unit cell consists of a local order of (1.15×1.15), in agreement with the STM observation.

Sometimes the $(\sqrt{31} \times \sqrt{31})R(\pm 9°)$ structure[36] coexisting with the hexagonal structure was seen from the

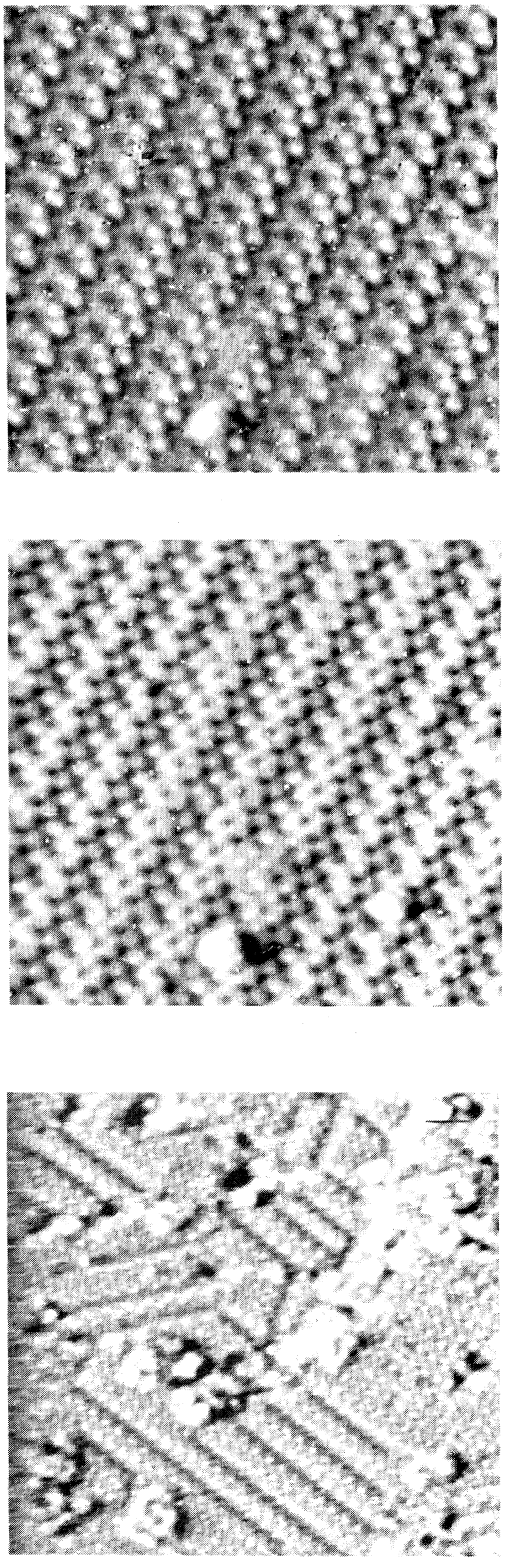

FIG. 1. (a) and (b) STM images (148 Å × 148 Å) of the striped phase (Ref. 37) with an In coverage of 0.3 ML; (a) empty-state image (1500 mV, 0.6 nA); (b) filled-state image (−1500 mV , 0.6 nA). (c) Empty-state STM image (148 Å × 148 Å, 1500 mV, 0.6 nA) of the striped phase with an In coverage of 0.1 ML.

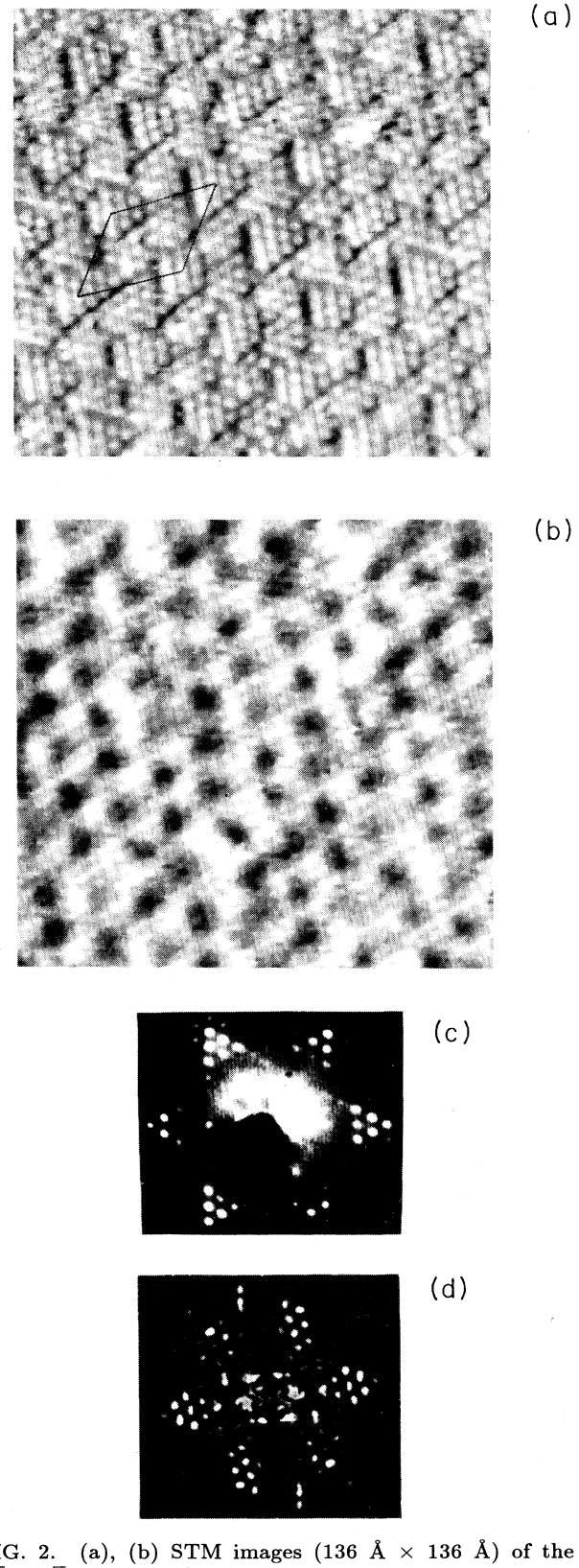

FIG. 2. (a), (b) STM images (136 Å × 136 Å) of the $(4\sqrt{3}\times4\sqrt{3})$ $R30°$ structure [hexagonal structure (Ref. 37)]; (a) empty-state (2500 mV, 20 nA) image with a $(4\sqrt{3}\times4\sqrt{3})$ unit cell superimposed on; (b) filled state (−2500 mV, 20 nA). (c) LEED pattern (51 V) of the structure. (d) FFT of (a).

surface. STM images along with a local-barrier-height image of the $(\sqrt{31}\times\sqrt{31})R(\pm 9°)$ structure are shown in Fig. 3. From these images we see the following features. (i) The $(\sqrt{31}\times\sqrt{31})$ structure is rotated by an angle of 9° from the substrate orientation. (ii) Each $(\sqrt{31}\times\sqrt{31})$ unit cell consists of two triangles. (iii) One of them consists of ten bright spots and the other only six. (iv) The bright spots in both triangles are aligned along the unit vectors of the $(\sqrt{31}\times\sqrt{31})$ structure, rather than parallel to the substrate unit vectors. (v) There is a less bright spot at the center of each corner hole. (vi) From the local-barrier-height image it is clear that the electronic structure of the triangles is quite different from that of the boundary. (vii) The surface, compared with the coexisting $(4\sqrt{3}\times4\sqrt{3})$ structure [Fig. 3(a)], is better ordered.

When the In coverage was higher than 0.8 ML only *mediocre* (4 × 4) LEED patterns [Fig. 4(a)] were seen *no matter if the surface was annealed or not*, and the spots were not very sharp nor was the background very low, indicating a less well-ordered structure. At this In coverage range it was so difficult to keep the STM tip from being ruined by, probably, the extra In atoms moving around on the surface that we were not able to get any useful images. However, comparing the LEED intensity curves [Fig. 4(b)] obtained from the (4 × 4) structure with their counterparts from the $(4\sqrt{3}\times4\sqrt{3})$ structure, we believe that the two structures must have the same adsorbing site and very similar local structures or the (4 × 4) structure might only be a less well developed $(4\sqrt{3}\times4\sqrt{3})$ structure.

IV. DISCUSSION

A. The $(4\sqrt{3}\times4\sqrt{3})$ structure

On the basis of our own observations as well as those of previous papers[36,37] a concrete atomic structural model is proposed for the $(4\sqrt{3}\times4\sqrt{3})$ reconstruction and is given in Fig. 5. This model explains the following features of the reconstruction. (i) Under STM, each unit cell looks to consist of three similar groups. (ii) In the empty-state images each group contains about seven to ten bright features arranged in a local order of about (1.15 × 1.15) since, as in the case of Al substitutional atoms on Si(111),[3] the empty states (around 2 eV) of the In substitutional atoms are expected to be localized above them. (iii) In the filled-state images the contrast inside the groups is reversed compared to that in the empty-state images because the filled states (around −2 eV) are localized above the Ge atoms.[3] (iv) The group boundaries are dark in the empty-state images but bright in the filled-state images as the (filled) dangling bonds (DB) exist only in the boundaries. (v) The model contains 27 In atoms, thus corresponding to an In coverage of 0.56 ML, in agreement with the experimental result. (vi) The surface exhibits a $(4\sqrt{3}\times4\sqrt{3})$ long-range order rather than a (4 × 4) order as a careful inspection of the model can tell that the three groups (including their

boundaries) in a unit cell are quite different from one another. (vii) Under STM the surface looks to be less well ordered as the In atoms at the corners of the groups (such as the one marked with a star) may, because of frustration,[43] jump back and forth between two neighboring locations belonging to two neighboring groups, respectively. Sometimes the surface may look like a (4 × 4) or even a "two-dimensional quasicrystal".[18] However, FFT's of such images still exhibit a quite nice ($4\sqrt{3} \times 4\sqrt{3}$) long-range order. (viii) With increasing coverages the size of the groups may increase a bit, thus resulting in reconstructions with similar structures but longer unit-cell lengths: β_1 to β_4 or the ($4\sqrt{3} \times 4\sqrt{3}$) to ($4.3\sqrt{3} \times 4.3\sqrt{3}$) reconstructions.[36] Actually, our STM images show that β_1 to β_4 coexist very often and the images in Fig. 2 were from a ($4.2\sqrt{3} \times 4.2\sqrt{3}$) area. However, for simplicity, in the present work we do not distinguish them and only use ($4\sqrt{3} \times 4\sqrt{3}$). Besides, this model is compatible with the ($4\sqrt{3} \times 4\sqrt{3}$) model of the effective scattering factors of "abnormal atoms" in Ref. 36, as well as the model qualitatively discussed in Ref. 37.

As for the driving force of the structure, it is well known that reduction of the DB density is the major motivation of surface reconstruction of semiconductors.[1] Now, in this model there are only 15 DB's in each ($4\sqrt{3} \times 4\sqrt{3}$) unit cell, i.e., 0.31 DB's per

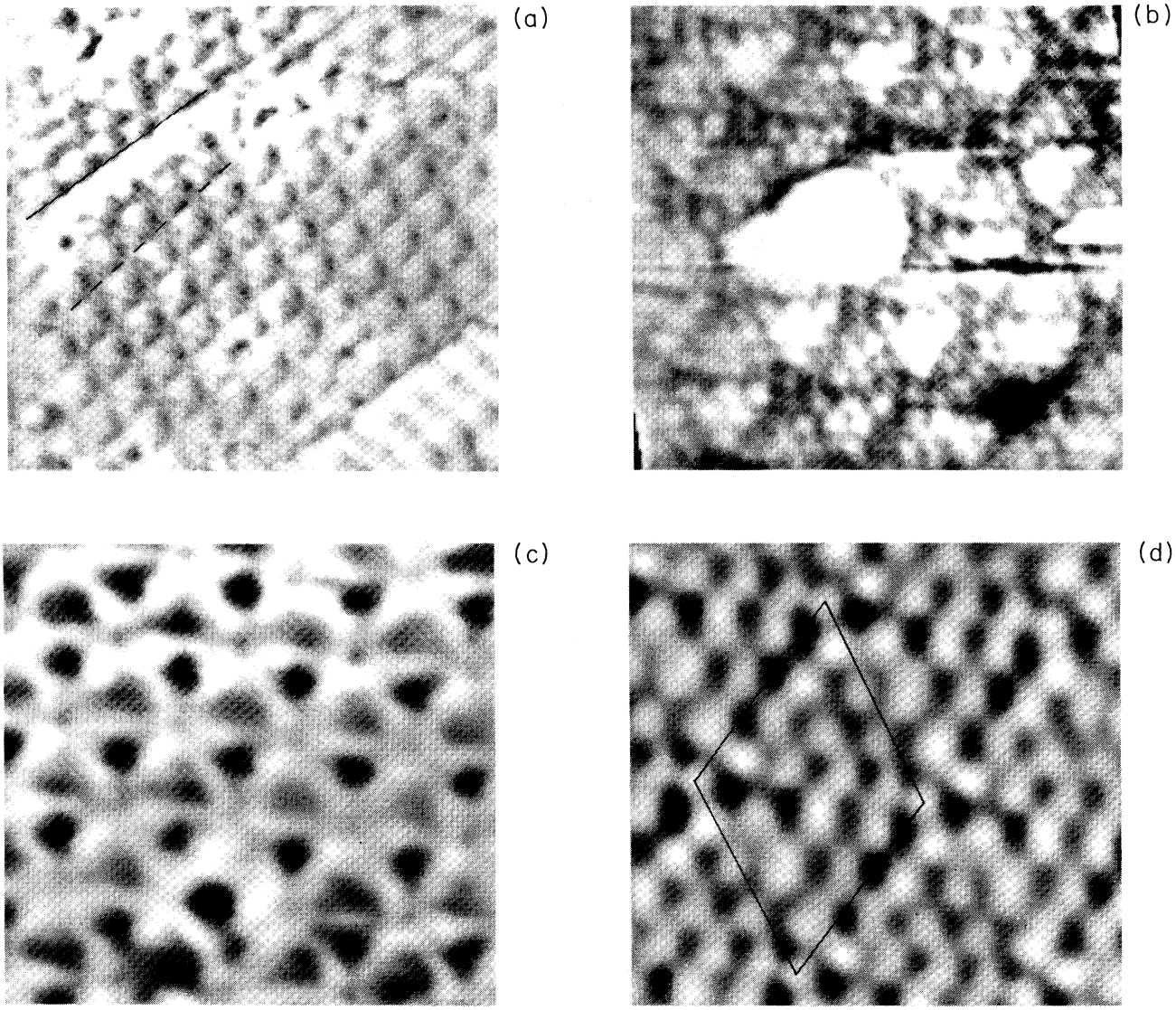

FIG. 3. (a) STM image (192 Å × 192 Å, 2500 mV, 1 nA) showing the ($\sqrt{31} \times \sqrt{31}$)$R(\pm 9°)$ structure (central area) coexisting with the ($4\sqrt{3} \times 4\sqrt{3}$) $R30°$ structure (upper left). The substrate and the ($\sqrt{31} \times \sqrt{31}$) orientations are indicated with solid and dashed line, respectively. The angle between them is 9°. (b) dc-mode STM image of the ($\sqrt{31} \times \sqrt{31}$)$R(\pm 9°)$ structure (87 Å × 87 Å, 1500 mV, 3 nA). (c) Local-barrier-height image of the structure (87 Å × 87 Å, tip height maintained with 1500 mV, 3 nA). (d) High-pass-filtered STM image of the structure (48 Å × 48 Å, 1500 mV, 5 nA), with a ($\sqrt{31} \times \sqrt{31}$) unit cell superimposed on the corner-hole-center atoms.

substrate unit cell, which is only slightly higher than 0.27 for the DAS structure of the Si(111)7×7 surface,[44] so that the model is very reasonable in this regard. Besides, stress relief is another very important factor, as shown by many recent works.[45–48] In this model there are 21 missing top-layer Ge atoms in each unit cell, so that there is plenty of room for relief of the compressive stress induced by In substitutional atoms, which have a larger covalent radius and three sp^2-like back bonds causing them to relax toward the substrate.

B. The $(\sqrt{31} \times \sqrt{31})R(\pm 9°)$ structure

Based upon our STM and local-barrier-height images as well as the careful observations of Ref. 36, a detailed structural model shown in Fig. 6 is proposed for the $(\sqrt{31} \times \sqrt{31})R(\pm 9°)$ structure. This model is able to explain features (i)–(vii) seen from the images shown in Fig. 3 and mentioned earlier. To understand these features one only needs to recall that the empty states are mainly localized above the In substitutional atoms, while the filled states are localized above the Ge atoms.[3] The STM feature (iv), i.e., the bright spots in both triangles are aligned along the unit vectors of $(\sqrt{31} \times \sqrt{31})$ instead of parallel to the substrate unit vectors, is not shown in the model for clarity. However, looking at the directions of the lateral bonds carefully, one may agree that the two triangles, under the tensile stress of these bonds, have a tendency to rotate clockwise so as to reduce the length of these bonds. As a result of this rotation, the In atom (bright spot) rows in the two triangles become parallel to the $(\sqrt{31} \times \sqrt{31})$ unit cell. To understand why the $(\sqrt{31} \times \sqrt{31})$ structure is better ordered than the $(4\sqrt{3} \times 4\sqrt{3})$, note that in this model the In substitutional atoms form two triangles while in the $(4\sqrt{3} \times 4\sqrt{3})$ model they

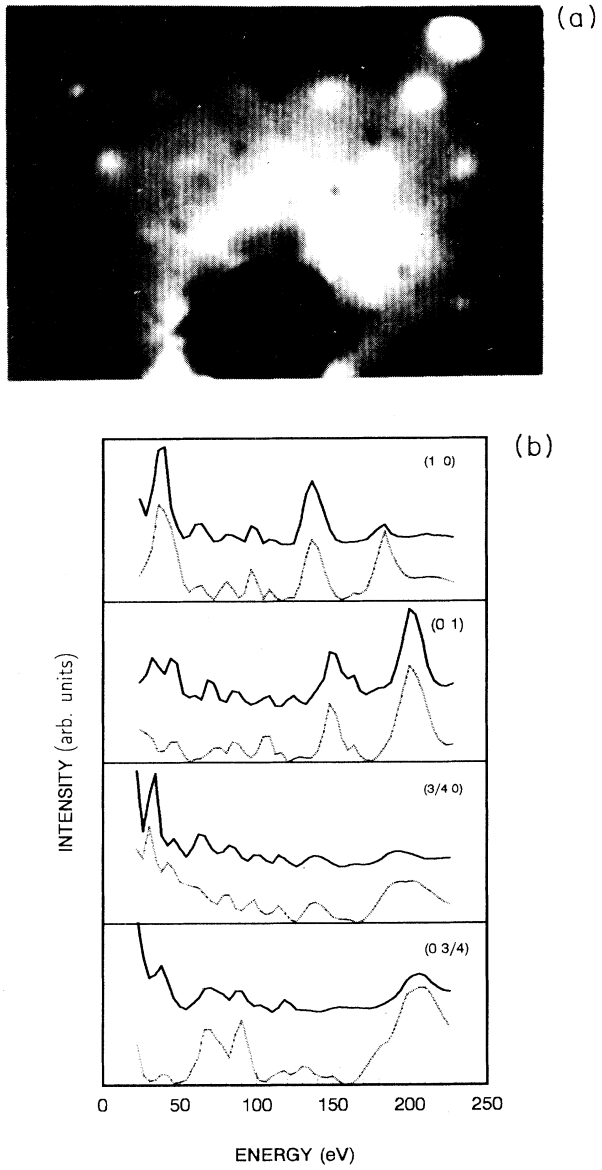

FIG. 4. (a) LEED pattern (24 V) of the (4 × 4) structure. (b) Comparison of the LEED (I-V) curves collected from the (4 × 4) structure (dashed curve) with their counterparts of the $(4\sqrt{3} \times 4\sqrt{3})$ structure (solid curve).

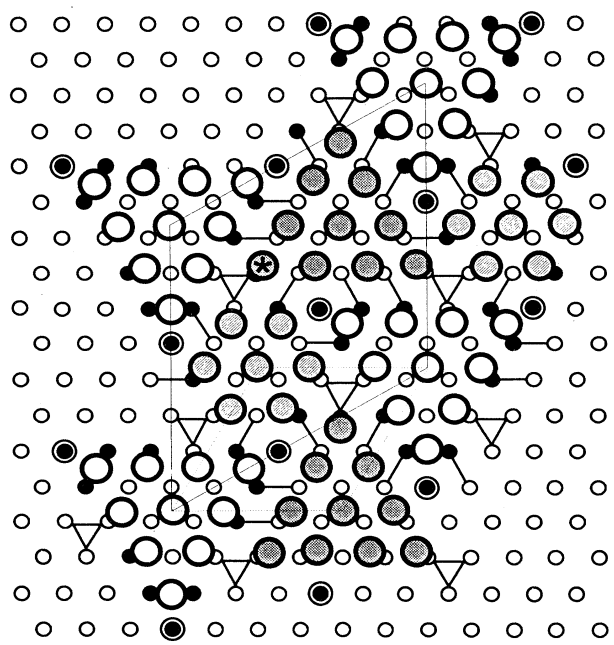

FIG. 5. Structural model proposed for the $(4\sqrt{3} \times 4\sqrt{3})$ structure. In this model some of the first-layer Ge atoms are missing and the rest are substituted by In atoms (large circle). For clarity, the In atoms in different groups are shaded differently (open, lightly shaded, and heavily shaded). The second-layer Ge atoms without (with) a DB are represented by an open (closed) small circle and are bonded either to an In atom or to each other by lateral bonds (bar), which are a result of rebonding and can reduce the number of broken bonds. Those third-layer Ge atoms that are visible from the top are represented by a closed circle with a ring and all have a DB because the second-layer Ge atom directly above them is missing. A unit cell of $(4\sqrt{3} \times 4\sqrt{3})$ and (4 × 4) is outlined with thin solid line and dashed line, respectively. For clarity, the second-layer Ge atoms are not shifted away from their bulk position as they are expected to in the real structure.

form two triangles and a hexagon. As we have mentioned, it might be just this hexagon that makes some of the In atoms frustrated and, thereby, the $(4\sqrt{3}\times 4\sqrt{3})$ surface less well ordered.

Besides, this model is compatible with all features of the $(\sqrt{31}\times\sqrt{31})$ structure pointed out by the earlier RHEED paper:[36] (i) The fact that the $(\sqrt{31}\times\sqrt{31})$ and $(4\sqrt{3}\times 4\sqrt{3})$ structures have almost identical In coverages (0.55 ML vs 0.56 ML) explains why upon different heat treatments the two structures can reversibly transform to each other.[36] (ii) The atomic arrangements of the two structures are considerably different from each other, thus explaining the very different RHEED intensities.[36] (iii) As the $(\sqrt{31}\times\sqrt{31})$ structure has a lower density of DB's (0.29 DB's per substrate unit cell) than 0.31 of the $(4\sqrt{3}\times 4\sqrt{3})$ structure, it is understandable why the latter, compared to the former, is metastable.[36] (iv) Since in the $(\sqrt{31}\times\sqrt{31})$ structure some In atoms have to substitute second-layer Ge atoms, it is not surprising that it needs a higher annealing temperature than that for the $(4\sqrt{3}\times 4\sqrt{3})$ structure.[36]

The model is actually very similar to the one proposed in Ref. 25 for In/Si(111), with the addition of the In corner atoms substituting Ge in the second layer. The reason for this addition is the following: (i) In the local-contrast-enhanced (or high-pass-filtered) empty-state images [Fig. 3(d)] there is a bright spot at the corners. (ii) In the dc-mode empty-state images [Fig. 3(b)] the corner spots are dimmer than those in the triangles (less clear but visible), thus indicating a lower position. (iii) In the local-barrier-height images [Fig. 3(c)] the corners, same as the triangles, are lower than the boundaries.

Clearly, the motivation of the $(\sqrt{31}\times\sqrt{31})$ structure is the same as that of the $(4\sqrt{3}\times 4\sqrt{3})$ structure, i.e., reduction of the density of the DB's and isotropic relief of the compressive stress induced by the In atom.

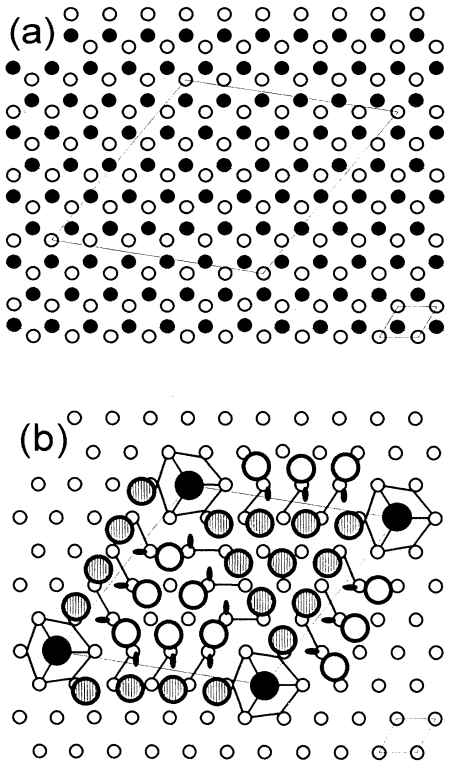

FIG. 6. (a) Schematic drawing of the truncated Ge(111) surface with a unit cell of $(\sqrt{31}\times\sqrt{31})R9°$ and (1×1) outlined. The closed and open circles represent the first- and second-layer Ge atoms, respectively. (b) Model of the $(\sqrt{31}\times\sqrt{31})R9°$ structure. In this model some of the first-layer Ge atoms are missing and the rest are substituted by In atoms (large open or shaded circle), thereby no first-layer Ge atoms remain. The second-layer Ge atoms (small circle) are bonded either to an In atom or to each other by lateral bonds (bar), a result of rebonding. The solid large circles represent the In atoms that substitute the second-layer Ge atoms, and thus are lower than the other In atoms. The solid ellipses represent the DB's. A unit cell of $(\sqrt{31}\times\sqrt{31})$ and (1×1) is also outlined. For clarity, the second-layer Ge atoms are not shifted away from their bulk position as they are expected to in the real structure.

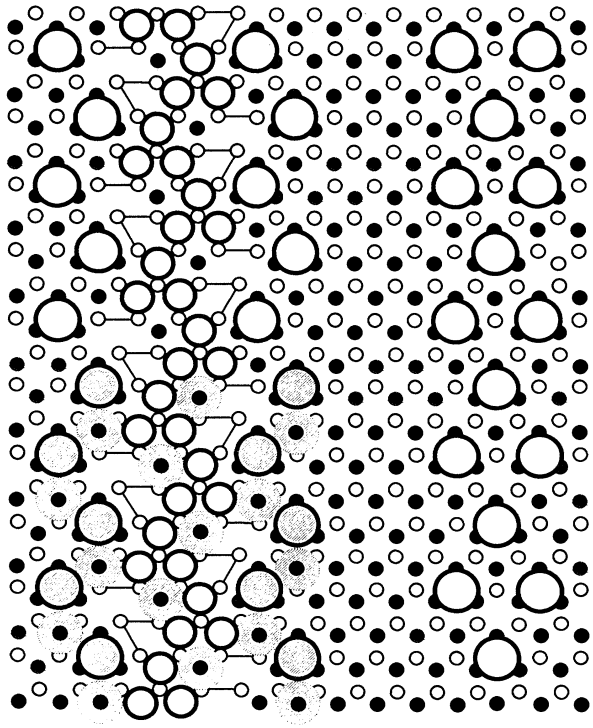

FIG. 7. Model of the striped structure. The large, closed small, open small, and medium circles represent the Ge adatoms, top-layer Ge atoms, second-layer Ge atoms, and In atoms, respectively. The stripe domains consisting of a variable number of $2\sqrt{3}$ rows of Ge adatoms are separated by domain walls, where some of the top-layer Ge atoms are substituted by In atoms and some of the second-layer Ge atoms are bonded to each other by lateral bonds (bar), a result of rebonding. For clarity, no atoms are shifted away from their bulklike positions although they are expected to in the real structure. For the same reason, in the right half of the figure only the bulk-like structure rather than the concrete domain wall structure is shown. The shaded areas in the lower-left half of the figure show where the bright features in the filled-state STM images are.

C. Structure of the striped phase

In view of the fact that the averaged width of the stripe domains increases with decreasing In coverage and that in these domains the (2×2) features are single in the empty-state images but twinned in the filled-state images, just as in the case of (2 × 2) domains on clean Ge(111) surfaces,[34,49,50] it has been concluded that the stripe domains consist of (2 × 2) Ge adatoms and rest atoms.[37] Our images support this conclusion. On the other hand, there has been no atomic model for the domain boundary structure, yet. However, it has been known that there could be neither Ge nor In adatoms in the boundaries and the In atoms there must be substitutional.[37] Besides, a model of the effective scattering factors of "abnormal atoms" has been proposed earlier.[36] According to these as well as the STM images we obtained, a concrete model for the striped phase is proposed and given in Fig. 7. The In coverage of this model is 0.30 ML [commensurate limit, i.e., when the domains have the minimal width of 8.0 Å (Ref. 37), in agreement with our own as well as previous experimental results.[36,37] According to what was mentioned at the beginning of this section the model is able to reproduce the features seen from both the empty-state and filled-state images of the stripe domains. Moreover, the model is also able to reproduce the features seen from the images of the domain boundaries, namely, in the filled-state images the DB's of the remaining top-layer Ge atoms give rise to single bright spots arranged in a local (2 × 2) order while in the empty-state images the In substitutional atoms, which have empty states localized above them,[3] give rise to a zigzag feature if they are not resolvable in an image. Since the Ge adatoms in the domains are higher than the In atoms in the boundaries the boundaries look darker than the domains in the empty-state images, although the In substitutional atoms also have empty states above them. In the filled-state images, however, as one would expect,[34,49,50] the features in the boundaries have about the same brightness as those in the domains do.

The model reflects the twofold motivation of the stripe phase: reduction of the DB density and stress relief. In the domain boundaries of the model the DB density is only 0.17 DB's per substrate unit cell. For the entire model surface it is 0.30, still much lower than 0.50 for the clean Ge(111)-$c(2\times8)$. Obviously, the lateral bonds among the second-layer Ge atoms can effectively release the unidirectional compressive stress.[37]

TABLE I. Comparison of medium-coverage reconstructions (Ref. 51) induced by group-III metals adsorbed on the (111) surface of group-IV semiconductors. Metal coverages in ML.

	Si(111)	Ge(111)
	Reconstruction: $\approx (7\times7)$ (Ref. 18); (8×8) (Ref. 21)	Reconstruction: $\approx (10\times10)$ (Ref. 32)
	Metal coverage: 0.5–1 (Refs. 2, 17, and 18); 0.5–0.6 (Ref. 21); ≈ 0.8 (Ref. 19)	Metal coverage: ≈ 1 (Ref. 32)
Al	Adsorption site: substitutional (Ref. 18)	Adsorption rate: unknown
	Inner structure: discommensurate (≈ 1.11) (Ref. 19)	Inner structure: discommensurate $\approx (1.04\times1.04)$ (Ref. 32)
	STM features (empty state): each unit cell consists of two "puckered" triangles separated by jagged troughs (Ref. 18)	STM features: (not available)
	Reconstruction: $\approx (6.3\times6.3)$ (Refs. 22 and 23); $\approx (5\pm5)\times(5\pm5)$ (Ref. 25)	Reconstruction: $\approx (8\times8)$, estimated from Fig. 4(b) in Ref. 37
	Metal coverage: ≈ 0.5 or higher (Refs. 24 and 25)	Metal coverage: ≈ 0.7 (Refs. 35 and 37)
	Adsorption site: substitutional (Ref. 24)	Adsorption site: substitutional (at very low coverages) (Ref. 33) (at ≈ 0.7 ML) (Refs. 35 and 37)
Ga	Inner structure: discommensurate (Ref. 23); $\approx (1\times1)$ (Ref. 25)	Inner structure: discommensurate (Refs. 35 and 37)
	STM features (empty state): internally ordered supercells with discrete boundaries (Ref. 23); quasiperiodic arrangement of triangular subunits containing spots in $\approx (1\times1)$ order (Ref. 25)	STM features (empty state): hexagonal domains consisting of essentially $\approx (1.09\times1.09)$ spots, separated by dark boundaries (Refs. 35 and 37)
	Reconstruction: $(\sqrt{31}\times\sqrt{31})$ (Ref. 26, 27, and 25)	Reconstruction: $(\sqrt{31}\times\sqrt{31})$ (Ref. 36) and $(4\sqrt{3}\times4\sqrt{3})$ (Refs. 36 and 37)
	Metal coverage: ≈ 0.5 (Ref. 26); 0.4–0.8 (Ref. 27); 0.5–0.7 (Ref. 25)	Metal coverage: $> 0.3-\approx 0.7$ (Refs. 36 and 37)
In	Adsorption site: unknown	Adsorption site: substitutional (Ref. 37)
	Inner structure: $\approx (1\times1)$ (Ref. 25)	Inner structure: discommensurate (Ref. 37) or incommensurate (Ref. 36)
	STM features (empty state): two triangular subunits in each unit cell, consisting of ten and six bright spots, respectively (Ref. 25)	STM features (empty state): hexagonal domains consisting of $\approx (1.25\times1.25)$ spots, separated by dark boundaries (Ref. 37)

D. A unified understanding of the III/IV(111) systems

So far, we have assumed that In atoms at the In/Ge(111) interfaces *substitute the top-layer Ge atoms* at all coverages and tend to relax downward because of the sp^2-like back bond formation, thus *causing a compressive surface stress.* To release the stress, *some of the top-layer Ge atoms may be missing and some new lateral bonds may form between the second-layer Ge atoms*, although the concrete way of stress relief (such as isotropic or unidirectional) may be different at different In coverages, thus resulting in quite different surface reconstructions. Obviously, Zegenhagen and co-workers believed that this reconstruction mechanism is common for the Ga/Ge(111) and In/Ge(111) systems when they were writing their recent In/Ge(111) paper.[37] To see if this mechanism really has a general validity, we made a careful survey (Table I) of the published papers concerning the reconstructions induced by about 0.5 ML of group-III metals adsorbed on the (111) surface of group-IV semiconductors. From Table I one can see that these reconstructions appear at very similar *coverage ranges*, have the group-III metal atoms substituting some topmost group-IV atoms and forming *discommensurate* (or *incommensurate*) clusters (or groups), and give rise to very similar STM images. So, we believe that this mechanism is a general model for group-III metals adsorbed on the (111) surface of group-IV semiconductors (at least for metal coverages around 0.5 ML). In fact, Hamers made an even more brave speculation: "such strain-related reconstructions near monolayer coverage for metals on Si may be a rather general phenomenon",[18] when he was comparing the Si(111)-(7× 7)-Al structure with the Si(111)-"5×5"-Cu structure.[43] Of course, *to prove the correctness of this unified understanding of the reconstruction mechanism of III/IV(111) systems, many further concrete and careful investigations are needed.*

One might have noticed that the reconstructions listed in Table I have quite different and even variable unit-cell sizes, rather than systematically varying with the covalent bond lengths of the relevant elements. However, there is nothing wrong with this. If these reconstructions are indeed motivated by the same mechanism as that of the In/Ge(111) system what one would expect is a systematic variation of the discommensurate cluster size rather than the unit-cell size. It has been known that, at least in the case of the $\approx(7\times7)$ reconstruction of Al/Si(111) (Ref. 18) and the $(\sqrt{31}\times\sqrt{31})$ reconstruction of the In/Si(111),[25] as well as the $(4\sqrt{3}\times4\sqrt{3})$ and $(\sqrt{31}\times\sqrt{31})$ reconstructions of In/Ge(111) shown in the present work, a unit-cell may consist of two or more incommensurate clusters. The mean cluster size should be more intrinsic, as indicated by the fact that the $(4\sqrt{3}\times4\sqrt{3})$ and $(\sqrt{31}\times\sqrt{31})$ reconstructions of the In/Ge(111) system have very similar mean cluster sizes [16 vs 15.5 substrate unit cells (suc)] though very different unit cell sizes (48 vs 31 suc). From Table I and the relevant references it can be deduced that the mean cluster size of the reconstructions is 100, 64, and 16 suc for the Al/Ge(111),[32] Ga/Ge(111),[37] and In/Ge(111) (Ref. 37 as well as present work) system, respectively; and 24.5 and 15.5 suc for the Al/Si(111) (Ref. 18) and In/Si(111) (Ref. 25) system, respectively. The data seem to indicate that the mean cluster size is closely related to the covalent radius of the metal as well as the semiconductor, i.e., the larger (smaller) the covalent radius of the metal (semiconductor) the smaller the cluster size. *To prove this eventually, many further concrete and careful investigations again are needed.*

V. SUMMARY

In summary, we have studied the surface reconstructions of the In/Ge(111) system by means of scanning tunneling microscopy, low-energy electron diffraction, and Auger electron spectroscopy, and have proposed that In atoms at the interface substitute the top-layer Ge atoms at all coverages and tend to relax downward because of their sp^2-like back bonds. The downward relaxation and the larger covalent radius of In atoms could give rise to a compressive surface stress. To release the stress, part of the top-layer Ge atoms may need to be removed. To reduce the number of the broken bonds introduced by removing of those Ge atoms, some new lateral bonds may form between those second-layer Ge atoms that otherwise would have broken bond(s). Depending on the concrete way of stress relief (such as isotropic or unidirectional), which may vary with the In coverage, different surface reconstructions may form. Detailed atomic structural models for the striped and hexagonal structures of the system have been proposed for further studies. Comparing the information gathered from previous papers concerning the systems of group-III metals adsorbed on (111) surfaces of group-IV semiconductors, we suggest that the above mechanism might be generally responsible for formation of the reconstructions in the III/IV(111) systems, at least for metal coverages around 0.5 ML.

ACKNOWLEDGMENTS

Sheng Fan is gratefully acknowledged for his important technical contribution. This work was supported by the National Natural Science Foundation of China and the Doctoral Program Foundation of the Education Ministry of China.

*Author to whom all correspondence should be addressed. Electronic address: wsyang@svr.bimp.pku.edu.cn

[1] See, e.g., L.P. LaFemina, Surf. Sci. Rep. **16**, 133 (1992), and references therein.
[2] J.J. Lander and J. Morrison, Surf. Sci. **2**, 553 (1964).
[3] J.R. Chelikowsky, Phys. Rev. B **16**, 3618 (1977).
[4] H.I. Zhang and M. Schlüter, Phys. Rev. B **18**, 1923 (1978).
[5] J.E. Northrup, Phys. Rev. Lett. **53**, 683 (1984).

[6]H. Nagayoshi, in *Dynamical Processes and Ordering on Solid Surfaces* (Springer-Verlag, Berlin, 1985).
[7]J.M. Nicholls, P. Mårtensson, G.V. Hansson, and J.E. Northrup, Phys. Rev. B **32**, 1333 (1985).
[8]G.V. Hansson, J.M. Nicholls, P. Martensson, and R.I.G. Uhrberg, Surf. Sci. **168**, 105 (1986).
[9]J.M. Nicholls, B. Reihl, and J.E. Northrup, Phys. Rev. B **35**, 4137 (1987).
[10]J. Nogami, Sang-il Park, and C.F. Quate, Phys. Rev. B **36**, 6221 (1987).
[11]J. Zegenhagen, J.R. Patel, P. Freeland, D.M. Chen, J.A. Golovchenko, and P. Bedrossian, Phys. Rev. B **39**, 1298 (1989).
[12]H. Huang, S.Y. Tong, W.S. Yang, H.D. Shih, and F. Jona, Phys. Rev. B **42**, 7483 (1990).
[13]J.M. Ricart, J. Rubio, and F. Illas, Phys. Rev. B **42**, 5212 (1990).
[14]D.M. Cornelison, C.S. Chang, and I.S.T. Tsong, J. Vac. Sci. Technol. A **8**, 3443 (1990).
[15]F. Illas, J.M. Ricrat, J. Casanovas, and J. Rubio, Surf. Sci. **275**, 459 (1992).
[16]J.C. Woicik, T. Kendelewicz, A. Herrera-Gomez, K.E. Miyano, P.L. Cowan, C.E. Bouldin, P. Pianetta, and W.E. Spicer, Phys. Rev. Lett. **71**, 1204 (1993).
[17]M. Kelly, G. Margaritondo, L. Papagno, and G.J. Lapeyre, Phys. Rev. B **34**, 6011 (1986).
[18]R.J. Hamers, Phys. Rev. B **40**, 1657 (1989).
[19]K. Nishikata, K. Murakami, M. Yoshimura, and A. Kawazu, Surf. Sci. **269-270**, 995 (1992).
[20]M. Yoshimura, T. Takaoka, T. Yao, T. Sato, T. Sueyoshi, and M. Twatsuki, *Chemical Surface Preparation, Passivation and Cleaning for Semiconductor Growth and Processing*, edited by R.J. Nemanich *et al.*, MRS Symposia Proceedings No. 259 (Materials Research Society, Pittsburgh, 1992), p. 157.
[21]A.V. Zotov, E.A. Khramtsova, S.V. Ryzhkov, A.A. Saranin, A.B. Chub, and V.G. Lifshits, Surf. Sci. **316**, L1034 (1994).
[22]M. Otsuka and T. Ichikawa, Jpn. J. Appl. Phys. **24**, 1103 (1985).
[23]D.M. Chen, J.A. Golovchenko, P. Bedrossian, and K. Mortensen, Phys. Rev. Lett. **61**, 2867 (1988).
[24]J. Zegenhagen, M.S. Hybertsen, P.E. Freeland, and J.R. Patel, Phys. Rev. B **38**, 7885 (1988).
[25]Sang-il Park, J. Nogami, and C.F. Quate, J. Microsc. **152**, 727 (1988).
[26]T. Aiyama and S. Ino, Surf. Sci. **82**, L585 (1979).
[27]M. Kawaji, S. Baba, and A. Kinbara, Appl. Phys. Lett. **34**, 748 (1979).
[28]N. Nakamura, K. Anno, and S. Kono, Surf. Sci. **256**, 129 (1991).
[29]M.S. Finney, C. Norris, P.B. Howes, and E. Vlieg, Surf. Sci. **277**, 330 (1992).
[30]H. Öfner, S.L. Surnev, Y. Shapira, and F.P. Netzer, Phys. Rev. B **48**, 10 940 (1993).
[31]H. Öfner, S.L. Surnev, Y. Shapira, and F.P. Netzer, Surf. Sci. **307-309**, 315 (1994).
[32]W.S. Yang and F. Jona, Solid State Commun. **42**, 49 (1982); W.S. Yang (unpublished).
[33]P. Molinàs-Mata and J. Zegenhagen, Phys. Rev. B **47**, 10 319 (1993).
[34]P. Molinàs-Mata, M. Böhringer, and J. Zegenhagen, Surf. Sci. **317**, 378 (1994).
[35]E. Artacho, M. Böhringer, P. Molinàs-Mata, J. Zegenhagen, G.E. Franklin, and J.R. Patel (to be published) (see Ref. 37); M. Böhringer, P. Molinàs-Mata, E. Artacho, and J. Zegenhagen (to be published) (see Ref. 37).
[36]T. Ichikawa, Surf. Sci. **111**, 227 (1981).
[37]M. Böhringer and J. Zegenhagen, Surf. Sci. **327**, 248 (1995).
[38]W.J. Huisman, M. Lohmeier, E. Vlieg and T.S. Turner (unpublished).
[39]R. Feidenhans'l, E. Landemark, M. Nielsen, D.M. Smilgies, J. Zegenhagen, L. Lottermoser, G. Falkenberg, L. Seehofer, and R.L. Johnson (unpublished).
[40]R.G. Zhao, J.F. Jia, and W.S. Yang, Phys. Rev. B **48**, 5333 (1993); Surf. Sci. Lett. **274**, L519 (1992).
[41]Zheng Gai, Hang Ji, Yi He, Chuan Hu, R.G. Zhao, and W.S. Yang, Surf. Sci. Lett. **338**, L851 (1995); Zheng Gai, Yi He, Hongbin Yu, and W.S. Yang, Phys. Rev. B **53**, 1042 (1995).
[42]J. Mou, J. Yan, W. Sun, W.S. Yang, C. Liu, Z. Zhai, Q. Xu, and Y. Xie, J. Vac. Sci. Technol. B **9**, 1566 (1991); J.X. Mou and W.S. Yang, Ultramicroscopy **42-44**, 1025 (1992).
[43]K. Mortensen, Phys. Rev. Lett. **66**, 461 (1991); J. Zegenhagen, E. Fontes, F. Grey, and J.R. Patel, Phys. Rev. B **46**, 1860 (1992).
[44]K. Takayanagi, Y. Tanishiro, M. Takahashi, and S. Takahashi, J. Vac. Sci. Tecnol. A **3**, 1502 (1985).
[45]C. Günther, J. Vrijmoeth, R.Q. Hwang, and R.J. Behm, Phys. Rev. Lett. **74**, 754 (1995).
[46]L.P. Nielsen, F. Besenbacher, I. Stensggaard, E. Lægsgaard, C. Engdahl, P. Stoltze, and J.K. Nørskov, Phys. Rev. Lett. **74**, 1159 (1995).
[47]E. Hahn, E. Kampshoff, N. Wälchli, and K. Kern, Phys. Rev. Lett. **74**, 1803 (1995).
[48]J.L. Stevenz and R.Q. Hwang, Phys. Rev. Lett. **74**, 2078 (1995).
[49]R.S. Becker, B.S. Swartzentruber, J.S. Vickers, and T. Klitsner, Phys. Rev. B **39**, 1633 (1989).
[50]E.S. Hirschorn, D.S. Lin, F.M. Leibsle, A. Samavar, and T.-C. Chiang, Phys. Rev. B **44**, 1403 (1991).
[51]The reconstructions considered here are only those that satisfy all the following conditions: existing after annealing (thus being stable); having no metal epitaxial layer; and best known. For the In/Si(111) system the $(\sqrt{7}\times\sqrt{3})$ (Ref. 25) and (4×1) reconstructions are not included as the former was not observed in Refs. 26 and 27 while the latter compared with $(\sqrt{31}\times\sqrt{31})$ may not be stable (Refs. 26 and 27) and, in addition, both are less known (Refs. 25–27). For the In/Ge(111) system the $(\sqrt{61}\times\sqrt{61})$ and (4.3×4.3) reconstructions are not included as they were reported only once (Ref. 36) and are less known, although both might be quite similar to $(4\sqrt{3}\times 4\sqrt{3})$ (Ref. 36).

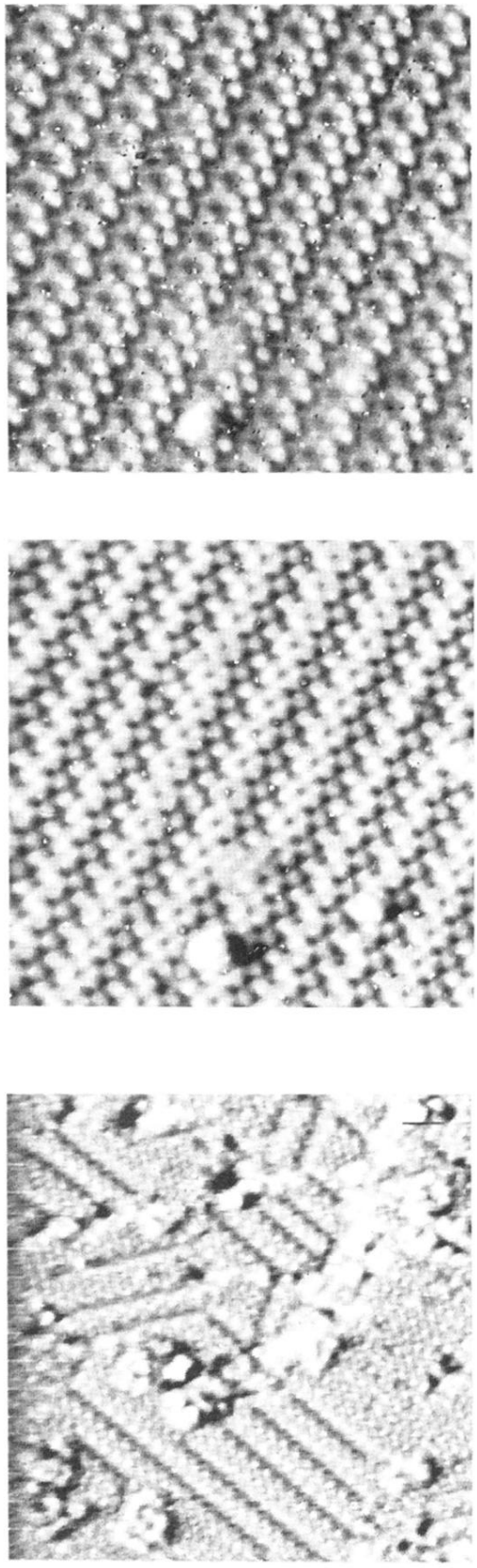

FIG. 1. (a) and (b) STM images (148 Å × 148 Å) of the striped phase (Ref. 37) with an In coverage of 0.3 ML; (a) empty-state image (1500 mV, 0.6 nA); (b) filled-state image (−1500 mV , 0.6 nA). (c) Empty-state STM image (148 Å × 148 Å, 1500 mV, 0.6 nA) of the striped phase with an In coverage of 0.1 ML.

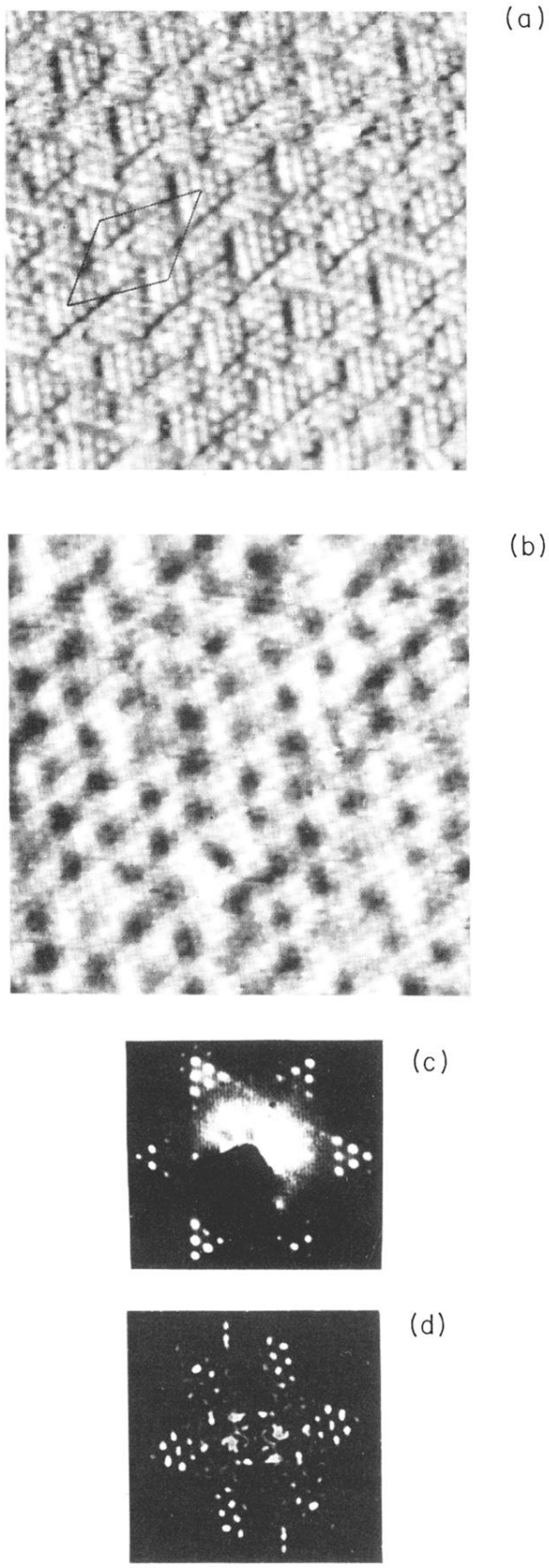

FIG. 2. (a), (b) STM images (136 Å × 136 Å) of the $(4\sqrt{3}\times4\sqrt{3})$ $R30°$ structure [hexagonal structure (Ref. 37)]; (a) empty-state (2500 mV, 20 nA) image with a $(4\sqrt{3}\times4\sqrt{3})$ unit cell superimposed on; (b) filled state (−2500 mV, 20 nA). (c) LEED pattern (51 V) of the structure. (d) FFT of (a).

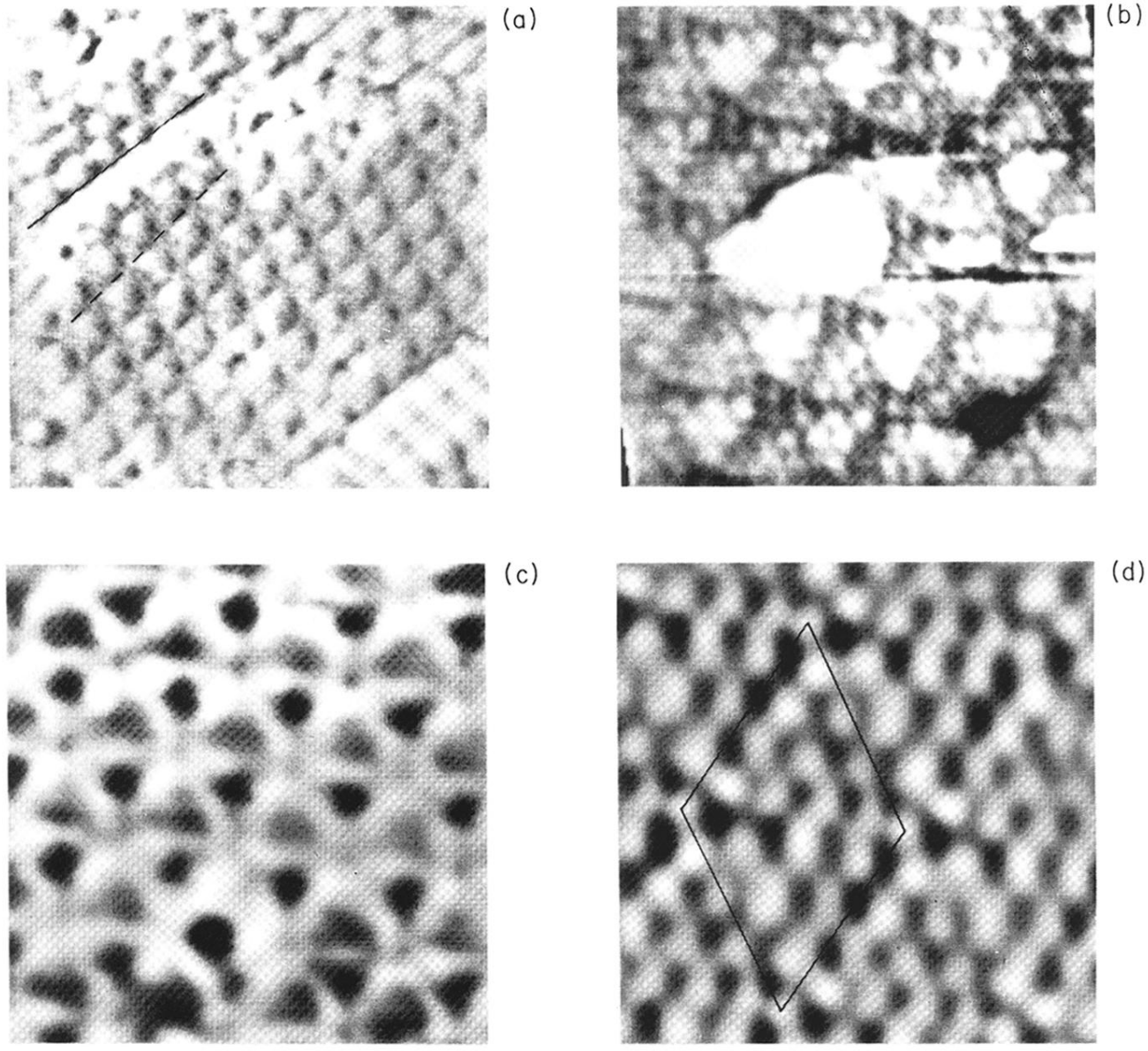

FIG. 3. (a) STM image (192 Å × 192 Å, 2500 mV, 1 nA) showing the $(\sqrt{31}\times\sqrt{31})R(\pm 9°)$ structure (central area) coexisting with the $(4\sqrt{3}\times 4\sqrt{3})$ $R30°$ structure (upper left). The substrate and the $(\sqrt{31}\times\sqrt{31})$ orientations are indicated with solid and dashed line, respectively. The angle between them is 9°. (b) dc-mode STM image of the $(\sqrt{31}\times\sqrt{31})R(\pm 9°)$ structure (87 Å × 87 Å, 1500 mV, 3 nA). (c) Local-barrier-height image of the structure (87 Å × 87 Å, tip height maintained with 1500 mV, 3 nA). (d) High-pass-filtered STM image of the structure (48 Å × 48 Å, 1500 mV, 5 nA), with a $(\sqrt{31}\times\sqrt{31})$ unit cell superimposed on the corner-hole-center atoms.

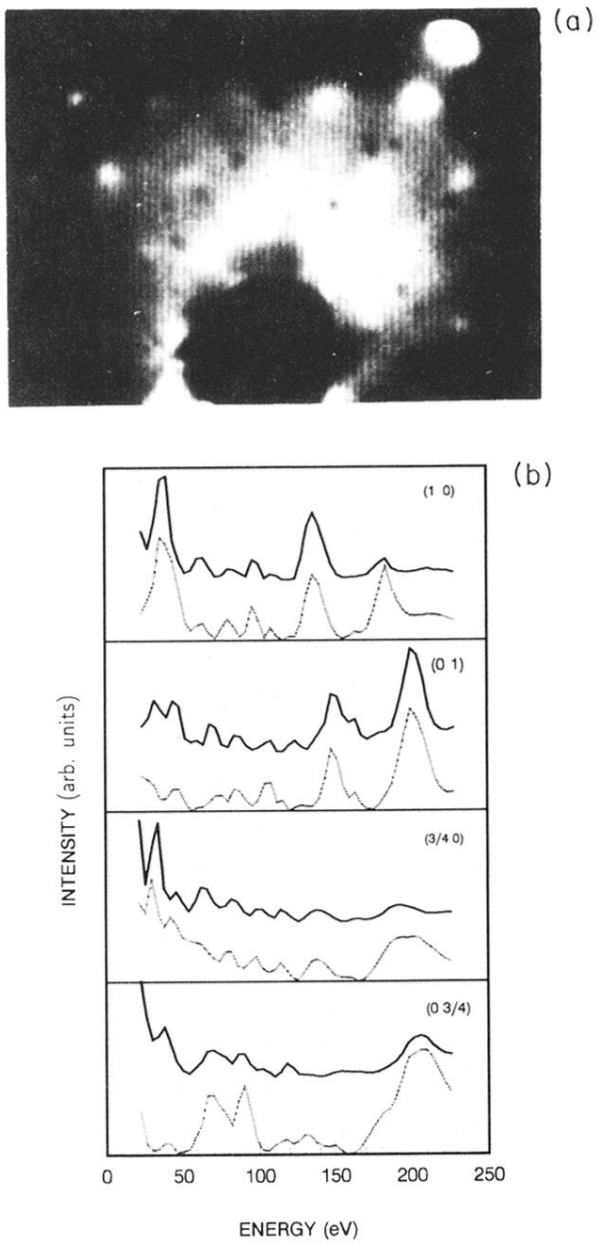

FIG. 4. (a) LEED pattern (24 V) of the (4×4) structure. (b) Comparison of the LEED (I-V) curves collected from the (4×4) structure (dashed curve) with their counterparts of the $(4\sqrt{3} \times 4\sqrt{3})$ structure (solid curve).